ACS APPLIED MATERIALS & INTERFACES

Research Article

www.acsami.org

Performance Improvement of Dye-Sensitized Solar Cells Using Room-Temperature-Synthesized Hierarchical TiO_2 Honeycomb Nanostructures

Fei Chu, Wei Li, Chunsheng Shi, Enzuo Liu, Chunnian He, Jiajun Li, and Naiqin Zhao*

School of Material Science and Engineering, and Tianjin Key Laboratory of Composite and Functional Materials, Tianjin University, Tianjin 300072, China

Supporting Information

ABSTRACT: Highly ordered hierarchical TiO_2 nanostructures involving primary honeycomb and secondary nanoparticles and nanowires are prepared by a two-step facile process. The TiO_2 nanotube arrays grow first on Ti foil through anodization. After the wet-chemical reaction of the TiO_2 nanotube arrays with alkaline and acid solution in turn, the hierarchical nanostructures wire-in-honeycomb and porous honeycomb are obtained by a dissolution−coagulation and dissolution−adsorption mechanism, respectively. The power conversion efficiency of the hierarchical TiO_2 honeycomb nanostructures for the dye-sensitized solar cells (DSCs) shows a significant improvement, as high as 5.73%, increased by 1.42 times compared with that of TiO_2 nanotube arrays. The performance improvement of DSCs based on the hierarchical nanostructures is attributed to the increase in the specific surface area.

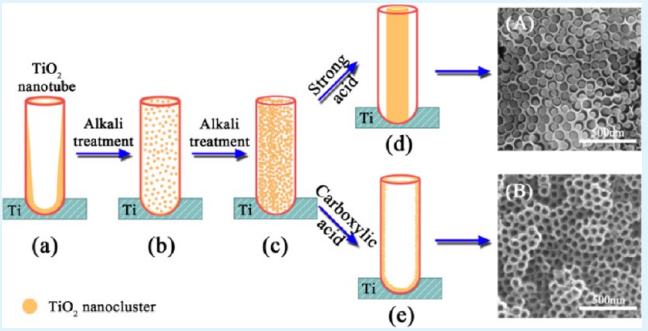

KEYWORDS: *hierarchical honeycomb nanostructure, titanium dioxide, photoanode, dye-sensitized solar cells*

1. INTRODUCTION

Novel nanosemiconductors have received considerable attention because of their potential applications in photovoltaics, photocatalysis, sensing, water splitting, and functional surface devices.[1−3] The physical and chemical properties of nanosemiconductor materials are determined by size, morphology, crystal phase, and dimensions. One-dimensional (1D) nanostructure applied to dye-sensitized solar cells (DSCs) can provide direct electron transport paths and reduce the electron recombination which is beneficial for the high efficiency of DSCs.[4−7] One of the semiconductor materials is titanium dioxide (TiO_2), which is a typical wide bandgap semiconductor (3.2 eV) and generally applied to gas sensors,[8,9] photocatalysis,[10,11] and DSCs.[12−18] Since the first report of TiO_2 nanotube (NT) arrays fabricated by electrochemical anodization,[19] various TiO_2 nanostructures have been synthesized such as nanorods,[20,21] nanowires,[22] nanobelts,[23] and coaxial arrays.[24−26]

Recently, the assembly of hierarchical array nanostructures has attracted wide concern owing to their special properties such as superior specific surface area, abundant and tunable multilevel interior structures, and multiphase anisotropic interfaces.[27−33] Zhuge et al. reported the preparation of TiO_2 nanoparticle/nanotube hierarchical structure, and the process involves TiO_2 nanowire as the template and hierarchical derivation to TiO_2 double-shell architecture.[34] Yang et al. prepared the highly oriented treelike TiO_2 arrays through a general acid vapor oxidation strategy.[35] Bae et al. successfully fabricated the multiwall anatase TiO_2 nanotubes by the deposition of alternating TiO_2/Al_2O_3 layer onto alumina templates.[29] However, owing to the structural complexity, developing the hierarchical TiO_2 nanostructure with controllable morphologies and high surface area still remains challenging. Therefore, it is desirable to find a simple, convenient, and low-cost approach to fabricating novel TiO_2 nanostructures in a facile reaction system.

Electrochemical anodization has been widely used as a facile and low-cost method for the preparation of oriented TiO_2 nanotube arrays. Recently, it was reported that wire-in-honeycomb could be obtained by treating TiO_2 nanotube arrays with KOH aqueous solutions and HCl in turn, and the HCl treatment which dissolves the cover layer on wire-in-honeycomb has no contribution to the formation of nanowires in the honeycomb.[36] In the present study, different acid treatments were studied in the fabrication of hierarchical TiO_2 nanostructures. It was found that the acid treatment plays an important role in the formation of different hierarchical TiO_2 nanostructures, such as TiO_2 hierarchical wire-in-honeycomb (WH) and porous honeycomb (PH). The advantage of the

Received: April 24, 2013
Accepted: July 23, 2013
Published: August 5, 2013

   dx.doi.org/10.1021/am401505t | ACS Appl. Mater. Interfaces 2013, 5, 7170−7175

hierarchical TiO_2 honeycomb nanostructures applied in DSCs was also investigated.

2. EXPERIMENTAL SECTION

2.1. Fabrication of Hierarchical TiO_2 Nanostructure. The fabrication of the hierarchical TiO_2 nanostructure includes two steps. In the first step, a pure titanium foil (≥99.9% purity, 0.5 mm thickness) was cleaned ultrasonically in deionized water, ethanol, and acetone in turn to remove any impurities. Subsequently, anodization was carried out in ethylene glycol ($C_2H_6O_2$) electrolyte containing 0.25% (in mass) NH_4F and 1% (in volume) H_2O at 50 V for 2h. The distance between the anode (Ti foil) and the cathode (Pt foil) was 3 cm. The obtained TiO_2 nanotube array (NTA) with Ti substrate was cleaned ultrasonically in ethanol for 20 min, and then dried under air atmosphere. In the second step, the TiO_2 NTA/Ti was immersed in 3 M KOH aqueous solution for 2 h. After rinsing in deionized water, the sample was immersed in 0.5 M HCl or CH_3COOH aqueous solution for 1h. Finally, the sample was cleaned ultrasonically in deionized water for 10 min to remove the residual covering layer above the hierarchical TiO_2 arrays. All of the experiments were carried out at room temperature. Some control experiments were also conducted for different time of acid treatment (HCl or CH_3COOH) to study the formation process of the hierarchical nanostructures. Other acid aqueous solutions such as H_2SO_4 (0.25M) and oxalic acid (0.25M) were further performed to understand the roles of acid treatment by similar process. All solvents above are analytically pure grade.

2.2. Fabrication of DSCs. The TiO_2 NTA/Ti substrate was annealed at 450 °C for 30 min with a heating and cooling rate of 10 °C min^{-1} under air atmosphere. The treated sample as a photoelectrode was then immersed into ethanol containing 0.5 mM N719 dye (*cis*-bis(isothiocyanato) bis(2,2′-bipyridyl -4,4′- dicarboxylato)-ruthenium-(II)-bis-tetrabutylammonium, Solaronix SA, Switzerland) in ethanol for 12h. After rinsing with ethanol and drying in an air atmosphere, the sensitized photoelectrode was assembled with a Pt-coated FTO separated by a Surlyn film (60 μm in thickness). Electrolyte was injected into the space by capillary action, which is composed of 0.1 M LiI, 0.1 M I_2, 0.6 M tetrabutylammonium iodide, and 0.5 M tert-butylpyridine in dry acetonitrile (Solaronix SA, Switzerland).[37,38]

2.3. Characterization. The morphology characteristics of the TiO_2 hierarchical arrays were observed using a field emission scanning electron microscope (FESEM, S-4800) and the transmission electron microscope (TEM, Tecnai G2 F20). Crystallization of the films was examined by X-ray diffraction (XRD, D/MAX-2500). The Brunauer–Emmett–Teller (BET) of TiO_2 hierarchical nanostructures were measured by Nitrogen adsorption isotherms at 77 K using an autosorb iQ instrument (Quantachrome U.S.). Dye amounts were measured by desorption in 0.1 M NaOH solution (H_2O:ethanol = 1:1) and absorbance was measured by a Hitachi 3010 spectrophotometer. The photocurrent (I) and photovoltage (V) of DSCs were measured by a Keithley 2400 SourceMeter under simulated sunlight AM 1.5 (100 mW cm^{-2}) produced by a solar simulator (Sciencetech-SS150).

3. RESULTS AND DISCUSSION

Images a and b in Figure 1 display the top-view and cross-section images of the TiO_2 nanotubes produced by the anodization process. The TiO_2 nanotube arrays have a relatively smooth surface. The nanotubes are about 80 nm in outer diameter, 76 nm in inner diameter, and 13 μm in length. After reacting with KOH for 2 h (Figure 1c, d), the nanotube film was transformed into two layers, in which the upper layer is a dense structure confirmed to be TiO_2 by XRD (see Figure S1 in the Supporting Information), and the lower layer is a full filling honeycomb structure which is formed by nanoclusters coagulation.[31] The nanotube wall of the lower layer is thicker than the as-anodized one, which indicates that the interior of the nanotubes has a V shape in accordance with previous observations.[39] The influence of two kinds of acid (HCl and

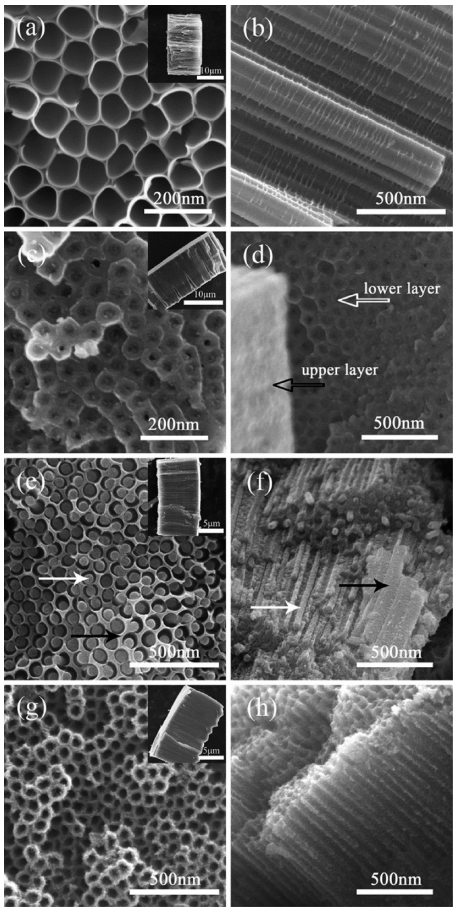

Figure 1. FESEM images of (a, b) the TiO_2 nanotube arrays, (c, d) TiO_2 arrays by alkali treatment, (e, f) the TiO_2 wire-in-honeycomb structure, and (g, h) the TiO_2 porous honeycomb structure. Insets in a, c, e, and g are the cross-section view images of each corresponding sample, the white and black hollow arrows indicate the lower layer and upper layer, and the white and black solid arrows indicate nanowires and honeycomb structures.

CH_3COOH) on the morphologies of the alkali treated TiO_2 NTA is compared, as shown in e, f and g, h in Figure 1, respectively. Images e and f in Figure 1 show the top-view and cross-section of the sample treated by HCl. It can be seen that a nanowire forms in the center of every honeycomb, which is named the hierarchical wire-in-honeycomb (WH). The honeycomb has an inner diameter of 75 nm, and the nanowires in the honeycomb have the average diameter of about 60 nm with a ~10 nm space from the wall. Images g and h in Figure 1 show the top-view and cross-section images of the sample treated by CH_3COOH. It is noticed that a porous honeycomb (PH) nanostructure with a ~20 nm porous wall and an inner diameter of ~40 nm appears instead of the WH structure by HCl treatment. Moreover, it seems that the wall consists of nanocrystalline which is in size of ~5 nm (Figure 1g). Meanwhile, the length (8 μm) of the two TiO_2 hierarchical arrays treated by alkaline and acid solution becomes shorter than that of the initial nanotube arrays as shown in the inserts of images c and e in Figure 1. The fact described above clearly indicates that acid treatment play an important role in fabricating different hierarchical TiO_2 honeycomb nanostructures.

Transmission electron microscopy (TEM) was used to further investigate the internal structures and morphology of

the amorphous hierarchical TiO_2 honeycomb nanostructures. The TEM image (Figure 2a) shows that it is a hollow nanotube

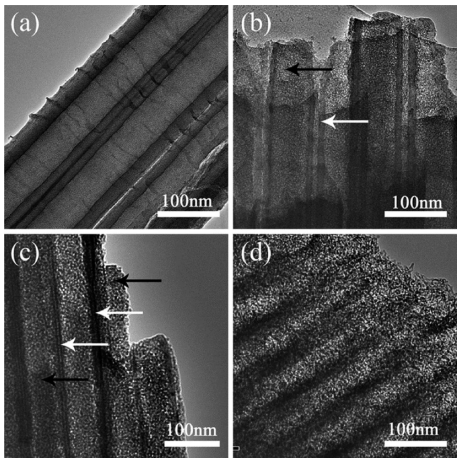

Figure 2. TEM images of (a) the TiO_2 nanotube arrays, (b) TiO_2 nanotube arrays by alkali treatment, (c) the TiO_2 wire-in-honeycomb structure, (d) the TiO_2 porous honeycomb structure; the white and black solid arrows indicate nanowires and honeycomb structures, respectively.

with a wall thickness of ~20 nm in the lower part. After reacting with KOH (Figure 2b), the walls of the nanotubes become thinner (~10 nm) and nanoclusters are formed in nanotubes, which can be ascribed to the partial dissolution of nanotube walls by KOH. After being treated with HCl (figure 2c), nanowires in the center of the tube are visible. However, most nanoclusters are still dispersed because of the ultrasonic preparation of TEM samples. Figure 2d reveals that CH_3COOH would make the nanoclusters adsorb on the wall, which results in nanotube wall thickening to ~20 nm. These are in good agreement with the above SEM result. The high-resolution TEM (HRTEM) of the newly formed nanostructures in Figure S2 in the Supporting Information indicates that the crystalline wall and the nanoclusters with 0.36 nm (101) lattice spacing are anatase crystals.

The formation process of the hierarchical TiO_2 honeycomb nanostructures were further investigated by time-dependent acid treatment. On prolonging the acid treatment time, the upper layer formed by KOH is dissolved and disappears (Figures 3 and 4). At the early stages of acid treatment, e.g., 1 min, the lower layer remains a fully filled honeycomb structure after immersing in CH_3COOH (Figure 5a) and HCl (Figure 5d). When the acid treatment time was prolonged to 10 min, the nanoclusters present different behavior. The nanoclusters also fully fill the tube with the action of CH_3COOH (figure 5b), whereas the nanoclusters are further precipitated in the central part of each tube by HCl treatment. A small space between the wire and the wall can be observed in Figure 5e. When the acid treatment time was prolonged to 30 min, the nanoclusters, with the action of CH_3COOH, were adsorbed on the wall and formed a porous honeycomb structure (Figure 5c). As for the HCl treatment, after reacting with HCl for 30 min (Figure 5f), the precipitation of nanoclusters further shrank, and a clear nanowire was formed in the honeycomb. The results further indicate that weak acid like CH_3COOH would impel the nanoclusters adsorb on the wall, whereas strong acid like HCl would impel the nanoclusters to precipitate and shrink.

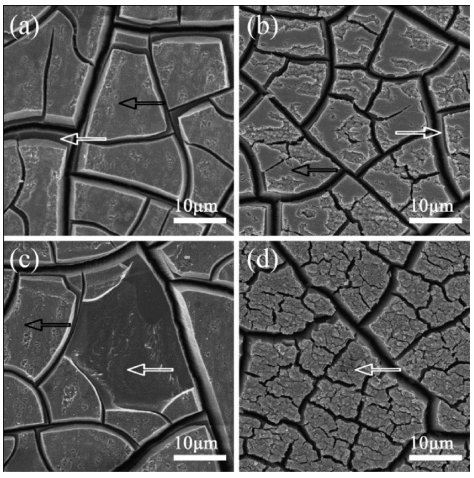

Figure 3. FESEM images of TiO_2 nanostructures prepared through further CH_3COOH treatment of TiO_2 nanotube arrays with different times of (a) 1, (b) 5, (c) 10, and (d) 30 min, the white and black hollow arrows indicate the lower layer and upper layer, respectively.

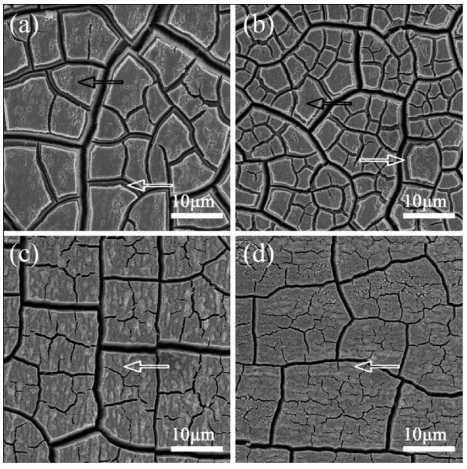

Figure 4. FESEM images of TiO_2 nanostructures prepared through further HCl treatment of TiO_2 nanotube arrays with different times of (a) 1, (b) 5, (c) 10, and (d) 30 min, and the white and black hollow arrows indicate the lower layer and upper layer, respectively.

Some related experiments were further performed to understand the roles of acid treatment in the fabrication of different nanostructures. According to the FESEM image (Figure 1c), TiO_2 nanoclusters precipitate after alkali treatment. As a result of H_2SO_4 treatment (Figure 6a), the nanoclusters shrink and the hierarchical WH nanostructures form, which is almost the same as HCl treatment. Furthermore, when oxalic acid is used, more TiO_2 nanoclusters are dissolved and fill in the honeycomb fully (Figure 6b), indicating that oxalic acid also has an effect on the dissociation of TiO_2 nanoclusters.

Figure 7 displays the XRD patterns of the NT fabricated by anodization (sample a), WH (sample b) fabricated by the KOH and HCl treatment of sample a, and PH (sample c) fabricated by the KOH and CH_3COOH treatment of sample a after annealing. The XRD patterns clearly indicate that all the crystal structures of the samples are anatase TiO_2 (JCPDS card No. 21−1272, *I*41/*amd*, a = 3.7852 Å, c = 9.5139 Å). Moreover, the sharp peaks reveal that the prepared TiO_2 nanostructures are well-crystallized, which is beneficial to the photoelectrode of DSCs.

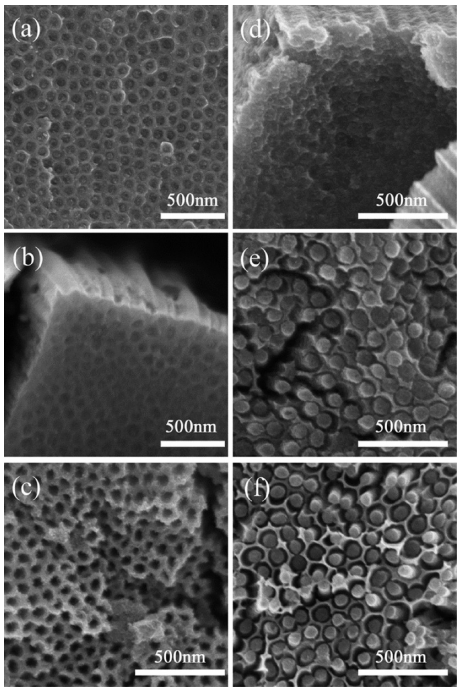

Figure 5. FESEM images of TiO_2 nanostructures prepared through further acid treatment of TiO_2 nanotube arrays with different times in CH_3COOH: (a) 5, (b) 10, and(c) 30 min; and in HCl: (d) 5, (e) 10, and (f) 30 min.

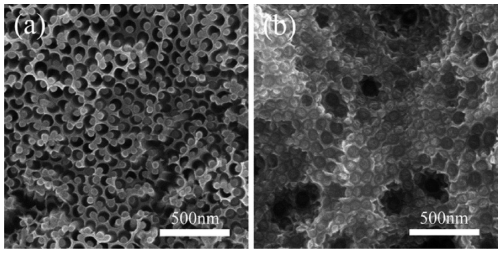

Figure 6. FESEM images of TiO_2 nanostructures prepared through different alkali treatment time and the treatment with different acid solutions, (a) H_2SO_4 (0.25M, 1 h) and (b) oxalic acid (0.25M, 1 h) after alkali treatment for 2 h.

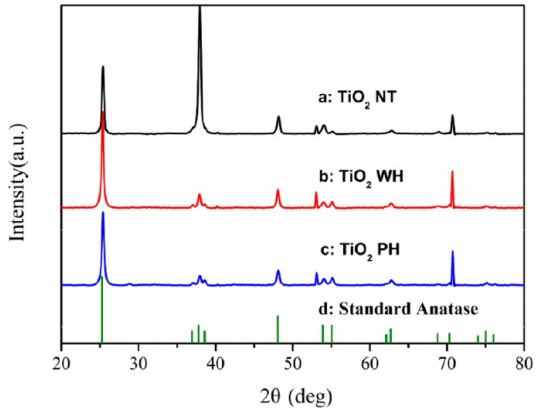

Figure 7. XRD patterns of the hierarchical TiO_2 arrays nanostructures after annealing at 450 °C for 30 min. (a) TiO_2 nanotubes, (b) TiO_2 wire-in-honeycombs, (c) TiO_2 porous honeycombs, (d) standard anatase.

Accordingly, the formation process of the hierarchical TiO_2 arrays nanostructures can be illustrated as Figure 8. It has been confirmed that the amorphous TiO_2 NT wall was partially destroyed by KOH and formed TiO_2 nanoclusters with Ti−OH groups on the surface (Figure 8b). Then the TiO_2 sol coagulated in the center of the honeycomb when the concentration reached the critical coagulation value (Figure 8c). When it was immersed in strong acid such as HCl and H_2SO_4, the surface of nanoclusters protonated forming $Ti-OH_2^+$.[40,41] These protonated surfaces easily combine with −OH groups of other TiO_2 nanoclusters to form Ti−O−Ti oxygen bridge bonds by eliminating a water molecule (Figure 8f). As a result, nanowires in the honeycomb are formed due to combination of TiO_2 nanoclusters (Figure 8d). In contrast, when it was immersed in weak acid such as CH_3COOH with −COOH group, the surface of TiO_2 nanoclusters and honeycomb wall easily absorb CH_3COOH molecule through hydrogen bond (Figure 8g).[40] Then the nanoclusters are absorbed to the wall of the honeycomb by physical adsorption forming the porous nanostructures (Figure 8e). Thus, it implies that the hierarchical TiO_2 nanostructures WH and PH were formed by a dissolution−coagulation and dissolution−adsorption process, respectively. On the basis of the above discussion, it indicates that acid treatment plays a key role in forming different hierarchical TiO_2 nanostructures.

Figure 9 shows the current−voltage characteristics of different DSCs fabricated by using as-anodized TiO_2 NT arrays, TiO_2 WH arrays, and TiO_2 PH arrays as photoelectrodes. The detailed photovoltaic parameters are summarized in Table 1. It should be noted that the film thickness of TiO_2 NT arrays is 13 μm, while for hierarchical PH and WH TiO_2 arrays, the film thickness is only 8 μm. Compared with TiO_2 NT arrays, the short circuit current density (J_{sc}) value of TiO_2 PH arrays shows a significant improvement from 7.09 to 17.31 mA cm^{-2}. The conversion efficiency (η) markedly increases from 2.37 to 5.73% and almost 1.42 times enhancement was achieved. The conversion efficiency of DSCs based on TiO_2 WH array photoelectrode also shows a significant enhancement of 74.3% compared to that of TiO_2 NT arrays, The superior conversion efficiencies of PH and WH arrays can be attributed to the higher absorption of the dye because of the larger surface area, as there is additional nanowire in the honeycomb of WH arrays and the coarse surface after dissolution-adsorption process in PH arrays. The results of the BET surface area analysis are summarized in Table 1. The BET surface area of WH and PH structures is 6.32 and 6.87 times higher than that of the NTA structure, respectively. With the enlarged surface area of hierarchical TiO_2 nanostructures, the dye adsorbed increases by 83 and 146% for WH structure and PH structure respectively, which correspond with the improvement of conversion efficiency. The increment of dye loading is not proportional to that of surface area, which indicates that not all surfaces are available to the dye molecules because of the small pore size of the hierarchical structure. Furthermore, the small space between the nanowire and the wall may partially hinder the access of the dye solution and the electrolyte to TiO_2 arrays. Optimal TiO_2 WH nanostructures remain to be studied further.

We have to point out that the conversion efficiency of our DSCs is inferior to the traditional ones based on TiO_2 nanocrystalline photoelectrodes, which is due to backside illumination of the novel nanostructure based on Ti substrate.[42] Therefore, we are currently working on preparing the novel

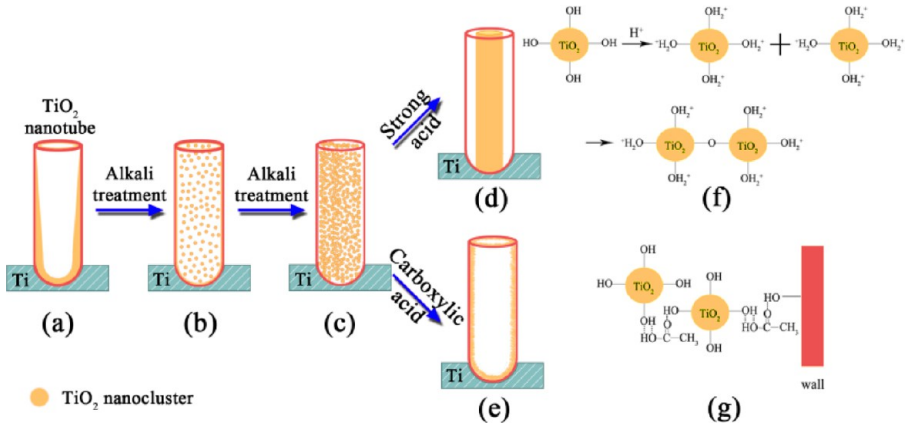

Figure 8. Schematic illustration of the formation process of the hierarchical TiO_2 nanostructures. (a) TiO_2 nanotube, (b, c) TiO_2 nanoclusters formed after alkali treatment, (d) TiO_2 wire-in-honeycombs, (e) TiO_2 porous honeycombs, (f) the reaction of nanoclusters in strong acid, (g) the reaction of nanoclusters in carboxylic acid.

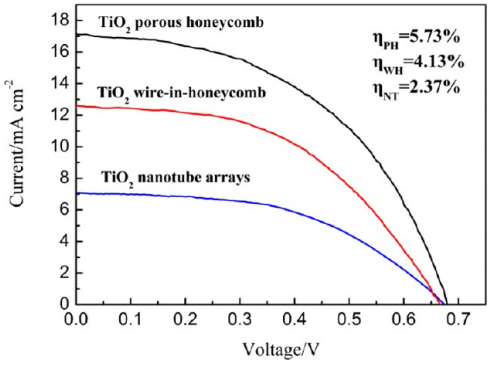

Figure 9. Photovoltaic parameters of the DSCs based on different TiO_2 arrays.

hierarchical nanostructure arrays on FTO glass to further improve the power conversion efficiency.

4. CONCLUSIONS

In summary, different highly ordered hierarchical TiO_2 honeycomb nanostructures have been successfully synthesized through a simple two-step approach, i.e., anodization and wet-chemical process. Through the research on the roles of acid treatment in the fabrication of TiO_2 nanostructures, it can be concluded that acid treatment play an important role in forming different hierarchical TiO_2 nanostructures, the strong acid could impel the nanoclusters forming nanowires, while weak acid could enhance the dissociation of TiO_2 nanoclusters and the formation of porous honeycomb nanostructure. Compared to the TiO_2 nanotube arrays, TiO_2 porous honeycomb arrays exhibited a significant increase on power conversion efficiency from 2.37 to 5.73% because of the larger specific surface area.

■ ASSOCIATED CONTENT

Supporting Information

Additional XRD patterns of TiO_2 structure prepared via alkali treatment and annealing at 450 °C for 30 min. TEM of hierarchical TiO_2 nanostructures after annealing at 450 °C for 30 min. This material is available free of charge via the Internet at http://pubs.acs.org/.

■ AUTHOR INFORMATION

Corresponding Author

*E-mail: nqzhao@tju.edu.cn.

Notes

The authors declare no competing financial interest.

■ ACKNOWLEDGMENTS

This work was supported by the Doctoral Programs Foundation of Ministry of Education of China (Grant 20120032110026).

■ REFERENCES

(1) Kuang, D.; Brillet, J. r. m.; Chen, P.; Takata, M.; Uchida, S.; Miura, H.; Sumioka, K.; Zakeeruddin, S. M.; Gratzel, M. *ACS Nano* **2008**, *2*, 1113−1116.
(2) Zheng, Q.; Zhou, B.; Bai, J.; Li, L.; Jin, Z.; Zhang, J.; Li, J.; Liu, Y.; Cai, W.; Zhu, X. *Adv. Mater.* **2008**, *20*, 1044−1049.
(3) Bai, H.; Liu, Z.; Sun, D. D. *Chem. Commun.* **2010**, *46*, 6542−6544.
(4) Kang, S. H.; Choi, S. H.; Kang, M. S.; Kim, J. Y.; Kim, H. S.; Hyeon, T.; Sung, Y. E. *Adv. Mater.* **2008**, *20*, 54−58.
(5) Kang, S. H.; Kim, H. S.; Kim, J. Y.; Sung, Y. E. *Nanotechnology* **2009**, *20*, 355307.
(6) Kim, J. Y.; Noh, J. H.; Zhu, K.; Halverson, A. F.; Neale, N. R.; Park, S.; Hong, K. S.; Frank, A. J. *ACS Nano* **2011**, *5*, 2647−2656.
(7) Lei, B. X.; Liao, J. Y.; Zhang, R.; Wang, J.; Su, C. Y.; Kuang, D. B. *J. Phys. Chem. C* **2010**, *114*, 15228−15233.

Table 1. Photovoltaic Characteristics of DSCs Based on Photoelectrodes of TiO_2 Nanotubes and Hierarchical TiO_2 Nanostructure Arrays and the Dye Amount Adsorbed by the Photoelectrodes

photoelectrode	V_{OC} (mV)	J_{SC} (mA cm^{-2})	FF (%)	η (%)	BET surface area (m^2 g^{-1})	dye adorbed (1×10^{-7}mol cm^{-2})
TiO_2 porous honeycomb	679	17.31	48.8	5.73	188	1.06
TiO_2 wire-in-honeycomb	669	12.42	49.7	4.13	175	0.77
TiO_2 nanotube	671	7.09	49.8	2.37	23.9	0.43

(8) Seo, M. H.; Yuasa, M.; Kida, T.; Huh, J. S.; Shimanoe, K.; Yamazoe, N. *Sens. Actuators, B* **2009**, *137*, 513−520.
(9) Kim, I. D.; Rothschild, A.; Lee, B. H.; Kim, D. Y.; Jo, S. M.; Tuller, H. L. *Nano Lett.* **2006**, *6*, 2009−2013.
(10) Fujishima, A.; Zhang, X.; Tryk, D. A. *Surf. Sci. Rep.* **2008**, *63*, 515−582.
(11) Asahi, R.; Morikawa, T.; Ohwaki, T.; Aoki, K.; Taga, Y. *Science* **2001**, *293*, 269−271.
(12) Sauvage, F.; Di Fonzo, F.; Li Bassi, A.; Casari, C. S.; Russo, V.; Divitini, G.; Ducati, C.; Bottani, C. E.; Comte, P.; Graetzel, M. *Nano Lett.* **2010**, *10*, 2562−2567.
(13) Yella, A.; Lee, H. W.; Tsao, H. N.; Yi, C.; Chandiran, A. K.; Nazeeruddin, M. K.; Diau, E. W. G.; Yeh, C. Y.; Zakeeruddin, S. M.; Gratzel, M. *Science* **2011**, *334*, 629−634.
(14) Snaith, H. J.; Schmidt-Mende, L. *Adv. Mater.* **2007**, *19*, 3187−3200.
(15) Li, L. L.; Tsai, C. Y.; Wu, H. P.; Chen, C. C.; Diau, E. W. G. *J. Mater. Chem.* **2010**, *20*, 2753−2819.
(16) Qiu, J. J.; Zhuge, F. W.; Lou, K.; Li, X. M.; Gao, X. D.; Gan, X. Y.; Yu, W. D.; Kim, H. K.; Hwang, Y. H. *J. Mater. Chem.* **2011**, *21*, 5062−5068.
(17) O'Regan, B.; Gratzel, M. *Nature* **1991**, *353*, 737−740.
(18) Gratzel, M. *Inorg. Chem.* **2005**, *44*, 6841−6851.
(19) Gong, D.; Grimes, C. A.; Varghese, O. K.; Hu, W. C.; Singh, R. S.; Chen, Z.; Dickey, E. C. *J. Mater. Res.* **2001**, *16*, 3331−3334.
(20) Liu, B.; Aydil, E. S. *J. Am. Chem. Soc.* **2009**, *131*, 3985−3990.
(21) Liao, J. Y.; Lei, B. X.; Chen, H. Y.; Kuang, D. B.; Su, C. Y. *Energy Environ. Sci.* **2012**, *5*, 5750−5757.
(22) Feng, X. J.; Shankar, K.; Varghese, O. K.; Paulose, M.; Latempa, T. J.; Grimes, C. A. *Nano Lett.* **2008**, *8*, 3781−3786.
(23) Shao, F.; Sun, J.; Gao, L.; Yang, S.; Luo, J. *J. Phys. Chem. C* **2011**, *115*, 1819−1823.
(24) Qiu, J.; Zhuge, F.; Li, X.; Gao, X.; Gan, X.; Li, L.; Weng, B.; Shi, Z.; Hwang, Y. H. *J. Mater. Chem.* **2012**, *22*, 3549−3554.
(25) Gu, D.; Baumgart, H.; Abdel-Fattah, T. M.; Namkoong, G. *Acs Nano* **2010**, *4*, 753−758.
(26) Albu, S. P.; Ghicov, A.; Aldabergenova, S.; Drechsel, P.; LeClere, D.; Thompson, G. E.; Macak, J. M.; Schmuki, P. *Adv. Mater.* **2008**, *20*, 4135−4139.
(27) John, S. E.; Mohapatra, S. K.; Misra, M. *Langmuir* **2009**, *25*, 8240−8247.
(28) Jung, J. H.; Shimizu, T.; Shinkai, S. *J. Mater. Chem.* **2005**, *15*, 3979−3986.
(29) Bae, C.; Yoon, Y.; Yoo, H.; Han, D.; Cho, J.; Lee, B. H.; Sung, M. M.; Lee, M.; Kim, J.; Shin, H. *Chem. Mater.* **2009**, *21*, 2574−2576.
(30) Wu, W. Q.; Lei, B. X.; Rao, H. S.; Xu, Y. F.; Wang, Y. F.; Su, C. Y.; Kuang, D. B. *Sci. Rep* **2013**, *3*, 1352.
(31) Rawolle, M.; Niedermeier, M. A.; Kaune, G.; Perlich, J.; Lellig, P.; Memesa, M.; Cheng, Y. J.; Gutmann, J. S.; Muller-Buschbaum, P. *Chem. Soc. Rev.* **2012**, *41*, 5131−5142.
(32) Liao, J. Y.; Lei, B. X.; Kuang, D. B.; Su, C. Y. *Energy Environ. Sci.* **2011**, *4*, 4079−4085.
(33) Orilall, M. C.; Wiesner, U. *Chem. Soc. Rev.* **2011**, *40*, 520−535.
(34) Zhuge, F. W.; Qiu, J. J.; Li, X. M.; Gao, X. D.; Gan, X. Y.; Yu, W. D. *Adv. Mater.* **2011**, *23*, 1330−1334.
(35) Yang, X. F.; Zhuang, J. L.; Li, X. Y.; Chen, D. H.; Ouyang, G. F.; Mao, Z. Q.; Han, Y. X.; He, Z. H.; Liang, C. L.; Wu, M. M.; Yu, J. C. *Acs Nano* **2009**, *3*, 1212−1218.
(36) Li, W.; Li, J.; Shi, C.; Liu, E.; He, C.; Du, X.; Zhao, N.; Springborg, M.; Dong, Y. *J. Mater. Chem.* **2012**, *22*, 13820−13825.
(37) Shao, F.; Sun, J.; Gao, L.; Yang, S.; Luo, J. *J. Phys. Chem. C* **2011**, *115*, 1819−1823.
(38) Lin, C. J.; Yu, W. Y.; Chien, S. H. *J. Mater. Chem.* **2010**, *20*, 1073−1077.
(39) Albu, S. P.; Ghicov, A.; Aldabergenova, S.; Drechsel, P.; LeClere, D.; Thompson, G. E.; Macak, J. M.; Schmuki, P. *Adv. Mater.* **2008**, *20*, 4135−4139.
(40) Yin, H.; Wada, Y.; Kitamura, T.; Kambe, S.; Murasawa, S.; Mori, H.; Sakata, T.; Yanagida, S. *J. Mater. Chem.* **2001**, *11*, 1694−1703.
(41) Yanagisawa, K.; Ovenstone, J. *J. Phys. Chem. B* **1999**, *103*, 7781−7787.
(42) Kang, M. G.; Park, N. G.; Ryu, K. S.; Chang, S. H.; Kim, K. J. *Sol. Energy Mater. Sol. Cells* **2006**, *90*, 574−581.